XLVI CILAMCE
VITÓRIA - ES - BRAZIL - 2025
XLVI IBERO-LATIN AMERICAN CONGRESS ON COMPUTATIONAL METHODS IN ENGINEERING

Capillary condensation in porous media considering a phase transition multiphase model

Marcelo A. Fogiatto[1], Nathan Mendes[1], Paulo C. Philippi[1]

[1]*Pontifical Catholic University of Parana – PUCPR*
Imaculada Conceição 1155, 80215-901, Curitiba, Brazil
m.a.fogiatto@gmail.com, nathan.mendes@pucpr.br, philippi@lmpt.ufsc.br

Abstract. Capillary condensation in building porous materials and the correct understanding of its underlying physics, leading to the enhancement of vapor transfer at low moisture contents, is a challenging research theme. In porous constrictions, the adsorbed moisture onto the solid surfaces of a porous material can grow around these surfaces, leading to what we know as capillary condensation: these constrictions are filled with liquid and, in consequence, form bridges, enhancing vapor diffusion through the porous material. Capillary condensation, thus, results from the intermolecular attraction forces between the vapor and the liquid molecules that are adsorbed onto the solid surfaces around constrictions. Vapor sorption has been modeled for materials presenting high hygroscopicity by considering the thermodynamic stability conditions of two-phase systems in single cavities of simple geometry, such as cylinders or spheres (Philippi et al. [1], Dutra et al. [2]). The continuous development of more rigorous molecular-based models of fluid systems, together with advances in computational resources, has resulted in an improved understanding of the underlying physics of these systems. In this study, an isothermal multiphase lattice-Boltzmann model with phase transition (Siebert et al. [3]) is used to simulate vapor condensation on the surface of a pore constriction represented by the spacing between two spheres (or cylinders in a two-dimensional simulation). The spacing between the solid bodies dictates if the liquid layers adhered to the walls give rise to capillary condensation. The results tend to agree with the Young-Laplace law.

Keywords: lattice-Boltzmann method, multiphase flow, porous medium, building physics, capillary condensation.

1 Introduction

A variety of factors, including an increase in environmental concerns across the past half century, has elevated the importance of efficient use of energy in buildings to new heights. Among the main topics of study related to it, moisture transfer through the building envelope is a critical one. Some of the lines of research are the ones related to the effect of humidity in the building envelope and the ones that concern how the moisture and heat transfer can affect building's performance from the energy consumption point of view.

As Janssen [4] points out, several tools for numerical simulation of moisture transfer in buildings have been developed in the past decades, including systems for simulation of thermal performance of whole buildings. In this kind of system – although being useful and able to reach good accuracy levels – the phenomena that take place inside the envelope itself is often overlooked or simplified, especially what can be perceived only at a diminutive space scale. An analysis of such phenomena – for example: what occurs in a porous medium in the presence of moisture – could contribute to better understand results obtained in the above-mentioned systems.

Great part of the materials used for building envelopes presents a porous structure. Assuming that humidity, when present, is adsorbed by the solid surfaces of the porous medium, a layer of saturated liquid can grow around these surfaces. Once liquid layers growing from different surfaces touch each other, capillary condensation takes place. To simulate this kind of situation, it is required a multiphase flow model that includes condensation. At least five kinds of models for condensation in general were reviewed by Szijártó et al. [5].

In the case of condensation in porous media, Gatica et al. [6] presented a simple model, but able to simulate

the process for media formed by solid cylinders under different porosities. Salinger and Frink [7] have presented algorithms to simulate condensation in parallel slit pores and in a domain containing equally spaced cylinders and, in other research, Shahraeeni and Or [8] have developed analytical models to simulate adsorption and condensation in wedge-shaped pores, as a step to understand these phenomena in rough sand grains, comparing the results to experimental ones.

In fluid dynamics in general, different approaches may be taken to solve problems, besides the traditional macroscopic approach. The microscopic one, including molecular simulation models, has the main disadvantage of high computational cost. Between these two, lies the mesoscopic approach. Within this approach, the lattice-Boltzmann method (LBM) is one of the most important and known methods. Among its main advantages regarding the subject of this study is the relative ease to deal with complex geometries, alongside a variety of multiphase models available, as the ones explained by Philippi [9].

With the pseudopotential multiphase model in the LBM, Sukop and Or [10] have simulated all the steps of capillary condensation for various geometries, including complex pore networks, and compared their results to analytical ones. Also employing such model, simulations of adsorption and capillary condensation in nanopores and nanochannels have been performed (Dou et al. [11], Sodagar-Abardeh et al. [12]). Using a sophisticated multi-component and multi-phase thermal model in LBM, Kazemian et al. [13] have investigated the interactions between air, vapor and liquid in media subject to capillary condensation. Li et al. [14] used the same model, however as a single component, to evaluate heat flux and evaporation in a porous structure.

Although the pseudopotential method has been widely used since its development by Shan and Chen [15], it presents some limitations, such as spurious currents, thermodynamic inconsistency, limited density and viscosity ratios, and an undesirable dependency between properties (Chen et al. [16]) – even though some of these problems have been mitigated in later studies. Thus, other solutions to LBM simulation of multiphase flows have been searched that can also be employed to capillary condensation in porous structures.

Stemming from the direct derivation of the lattice-Boltzmann equation from the continuous Boltzmann equation by He and Luo [17], studies – such as the ones by Philippi et al. [18] and Shan et al. [19] – have paved the way to simulate a wider range of phenomena using the LBM. This path led to a multiphase model with phase transition proposed by Siebert et al. [3]. In the present study, we aim to adapt and apply such model to simulate the fluid-solid and liquid-vapor interactions, trying to understand in which situations capillary condensation is more prone to take place, as well as its impact on the moisture transfer through the envelope.

2 The lattice-Boltzmann equation

A fundamental step to employ the LBM in each situation is to work with the lattice-Boltzmann equation (LBE), which can be written, in its dimensionless form, as

$$\frac{\partial \bar{f}_i}{\partial t^*} + \boldsymbol{e}_i \,.\, \bar{\nabla} \bar{f}_i = \bar{\Omega}_i \,, \tag{1}$$

where $\bar{f}_i$ represents the discrete distribution function, t^* the time, and $\boldsymbol{e}_i$ the discrete velocity for each direction denoted by i. The dimensionless gradient operator $\bar{\nabla}$ can be obtained by $h \times \nabla$, where h is the distance between two sites in the lattice. In this case, i = {0, 1, 2, …, 16} since the lattice chosen was the D2V17, developed by Philippi et al. [18], represented in Fig. 1. The particle interaction operator in each discrete direction, represented by $\bar{\Omega}_i$, is written as

$$\bar{\Omega}_i = \frac{\bar{f}_{eq,i} - \bar{f}_i}{\tau^*} + \boldsymbol{g}^* . (\boldsymbol{e_i} - \boldsymbol{u}^*)\, \bar{f}_{eq,i} \,, \tag{2}$$

where the first term on the right-hand side of eq. (2) is the model for collision of particles, known as the BGK collision operator, developed by Bhatnagar et al. [20]. The dimensionless relaxation time τ^* serves as a simulation parameter. It equals the ratio τ/δ, where δ is the simulation time-step. The second term is related to the force acting on the particles, where $\boldsymbol{g}^*$ represents their acceleration, and $\boldsymbol{u}^*$, the macroscopic flow velocity.

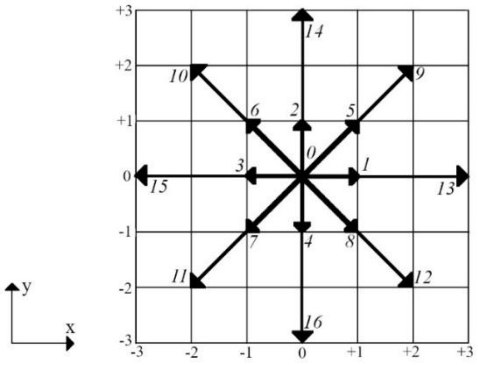


Figure 1. The D2V17 lattice

The equilibrium distribution function is represented by $\bar{f}_{eq,i}$ and, for the D2V17 lattice in an isothermal case, can be obtained by

$$\bar{f}_{eq,i} = \rho_r w_i \left[1 + a_s^2(\boldsymbol{e_i}.\boldsymbol{u}^*) + \frac{a_s^4}{2}(\boldsymbol{e_i}.\boldsymbol{u}^*)^2 - \frac{a_s^2(\boldsymbol{u}^*)^2}{2} + \frac{a_s^6}{6}(\boldsymbol{e_i}.\boldsymbol{u}^*)^3 - \frac{a_s^4(\boldsymbol{u}^*)^2}{2}(\boldsymbol{e_i}.\boldsymbol{u}^*)\right], \tag{3}$$

where ρ_r is the reduced density, which is calculated by the ratio ρ/ρ_c. The subscript c denotes a property at the critical point for a substance. The lattice scaling factor a_s and the values of the weight function w_i for different directions, as provided by Siebert et al. [21], are shown in Tab. 1.

Table 1. D2V17 weights and scaling factor

w_0	$[575+193(193)^{1/2}]/8100$
w_{1-4}	$[3355-91(193)^{1/2}]/18000$
w_{5-8}	$[655+17(193)^{1/2}]/27000$
w_{9-12}	$[685-49(193)^{1/2}]/54000$
w_{13-16}	$[1445-101(193)^{1/2}]/162000$
a_s	$\{5[25+(193)^{1/2}]/72\}^{1/2}$

Regarding the acceleration on eq. (2), one way to show it, not considering external body forces, is

$$\boldsymbol{g}^* = -\frac{\overline{\nabla}\left(P_r - P_{r,id}\right)}{P_{r,id}} + (\lambda^*)^2 \frac{\kappa^* a^*}{T_r}\,\overline{\nabla}\,\overline{\nabla}^2\rho_r\,, \tag{4}$$

where P_r represents the pressure obtained by the equation of state (EOS), $P_{r,id}$ the reduced ideal gas pressure, λ^* is the interface resolution, T_r the reduced temperature, κ^* and a^* the dimensionless surface parameter and EOS force parameter, respectively. Considering the van der Waals EOS, chosen to this study, a^* has the value of 9/8, and its dimensional form is given by $9kT_c/8n_c$, where n_c is the number density at the critical point and k, the Boltzmann constant.

The attainment of the remaining variables and properties from eq. (4) was carefully studied by Philippi [9]. One of them is the integral function

$$I = \int_{\rho_{r,l}}^{\rho_{r,v}} \sqrt{\psi^*_{exc}}\, d\rho_r\,. \tag{5}$$

Using the Maxwell area rule it is possible to obtain the saturation reduced densities of liquid $\rho_{r,l}$ and vapor $\rho_{r,v}$. And ψ^*_{exc} represents the dimensionless Helmholtz energy excess (HEE) along the interface for the EOS. Now, knowing that γ is the surface tension of a fluid at a given temperature, the surface parameter is calculated using

$$\kappa = \frac{\gamma^2}{2\,I^2\,n_c^2\,P_c}\,. \tag{6}$$

Once the values of these variables were obtained, and assuming a linear variation in the interface density profile,

besides knowing the value of HEE at the liquid-vapor interface middle point x_m, the interface thickness is calculated by

$$\lambda = n_c \sqrt{\frac{\kappa}{2\, P_c\, \psi^*_{exc}(x_m)}}\, \left(\rho_{r,l} - \rho_{r,v}\right). \tag{7}$$

The interface resolution λ^* is chosen keeping in mind the stability of the numerical model. Since a physical value for interface thickness is obtained, it is possible to calculate the distance between lattice sites as λ/λ^*. The only value left to obtain so eq. (4) can be used is the dimensionless surface parameter, given by

$$\kappa^* = \frac{\kappa}{a\, \lambda^2}. \tag{8}$$

3 Streaming term discretization and boundary conditions

Performing a Taylor-series expansion of the second order on eq. (1), its discrete form may be written as

$$\bar{f}_i(\boldsymbol{x}, t) = \bar{f}_i(\boldsymbol{x} - \boldsymbol{e}_i h, t - \delta) + \frac{1}{2}[\bar{\Omega}_i(\boldsymbol{x}, t) + \bar{\Omega}_i(\boldsymbol{x} - \boldsymbol{e}_i h, t - \delta)], \tag{9}$$

which is implicit on the interaction term. Siebert et al. [3] have solved this issue inserting the modified distribution

$$\tilde{f}_i(\boldsymbol{x} - \boldsymbol{e}_i h, t - \delta) = \bar{f}_i(\boldsymbol{x} - \boldsymbol{e}_i h, t - \delta) - \frac{1}{2}\bar{\Omega}_i(\boldsymbol{x} - \boldsymbol{e}_i h, t - \delta). \tag{10}$$

The streaming step may be performed for each direction of the lattice as

$$\tilde{f}_i(\boldsymbol{x}, \mathrm{t}) = \tilde{f}_i(\boldsymbol{x} - \boldsymbol{e}_i h, t - \delta) + \frac{1}{2}\bar{\Omega}_i(\boldsymbol{x} - \boldsymbol{e}_i h, t - \delta). \tag{11}$$

Subsequently, the original distribution $\bar{f}_i(\boldsymbol{x}, t)$ can be retrieved for each site at each time-step by

$$\bar{f}_i(\boldsymbol{x}, \mathrm{t}) = \tilde{f}_i(\boldsymbol{x}, t) + \frac{1}{2}\bar{\Omega}_i(\boldsymbol{x}, t - \delta). \tag{12}$$

Thus, the macroscopic properties for the current time-step in each site are calculated by

$$\rho_r(\boldsymbol{x}, \mathrm{t}) = \sum_i \bar{f}_i(\boldsymbol{x}, t), \tag{13 a}$$

$$u^*_x(\boldsymbol{x}, \mathrm{t}) = \frac{1}{\rho_r(\boldsymbol{x}, \mathrm{t})} \sum_i \bar{f}_i(\boldsymbol{x}, t)\, . e_{i,x}, \tag{13 b}$$

$$u^*_y(\boldsymbol{x}, \mathrm{t}) = \frac{1}{\rho_r(\boldsymbol{x}, \mathrm{t})} \sum_i \bar{f}_i(\boldsymbol{x}, t)\, . e_{i,y}. \tag{13 c}$$

These new properties enable the user to obtain the interaction term $\bar{\Omega}_i$ of the subsequent time-step. Using these data, the new modified distribution may be calculated by eq. (10) for each time-step at every lattice site. Then, the streaming step of eq. (11) is performed setting the iterative process on its course.

Regarding the simulation domain and its boundary conditions, it is a 2-D rectangular domain with initial ρ_r known for each fluid site, as it is for east and west borders. The north and south borders are periodic. In the interaction with the solids, the streaming step is treated with the half-way bounce-back approach. In the east and west borders, the approach used is similar to the one by Zou and He [22].

On the discretization and treatment of the gradient and laplacian of gradient present in eq. (4), the procedure followed was the same explained by Siebert et al. [3]. In the case of this study, situations arise where there is no fluid site at a given lattice vector distance. Therefore, for the east and west borders, the values of density and pressure that influence the gradients are those of the sites on the boundary. In the case of the fluid sites near solid walls, they are treated as influenced by saturated liquid density and saturation pressure. It comes from the assumption that there is always a minimal saturated liquid layer adhered to the solid surface.

4 Results

Considering a square domain, measuring 300x300 nm filled with fluid, containing two circles of 100 nm diameter acting as solid bodies, separated by at least 13 nm, simulations were executed in a T_r range from 0.82 to 0.89. It was performed in order to observe the geometry of the saturated liquid-vapor interface for different temperatures. Some of these results may be seen in Fig. 2.

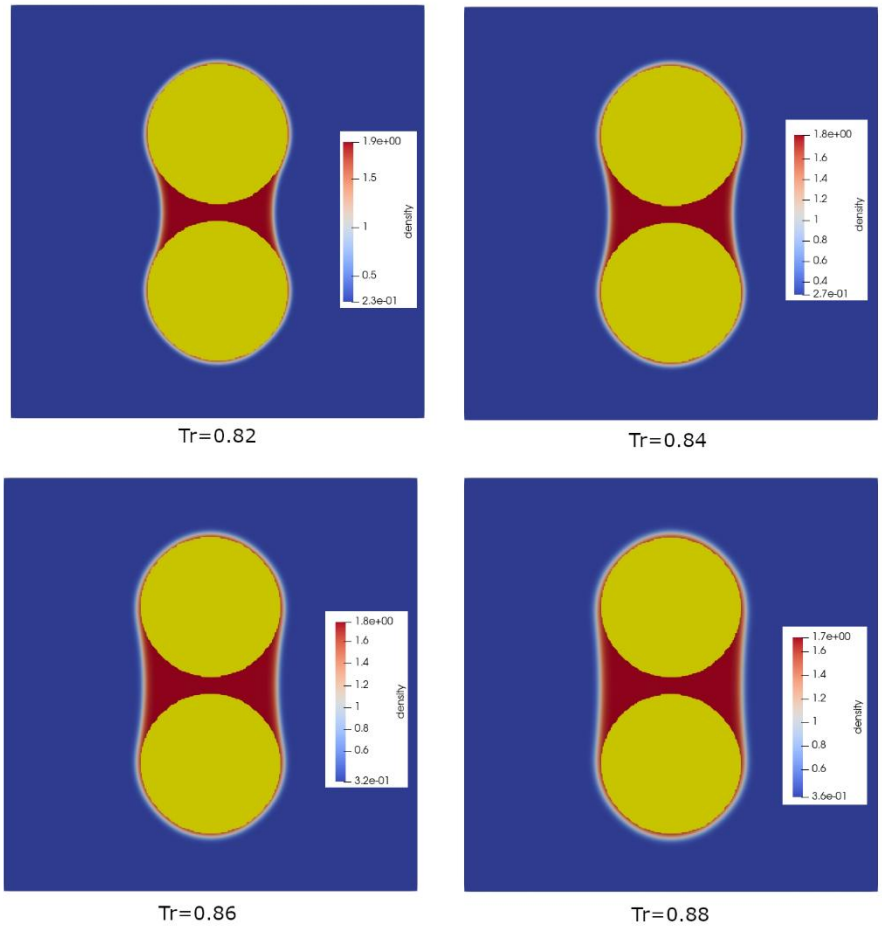


Figure 2. Liquid-vapor interface radius for different temperatures, in 300x300 nm domain and 100 nm diameter circles

Those simulations allow the reader to see the results through the lenses of the Young-Laplace law. Although the numerical values of interface radius expected from the Young-Laplace depend strongly on the particular geometry of each case, an inverse proportionality is always to be expected between the interface radius and the liquid/vapor density ratio. Such tendency may be observed in Fig. 3, remembering that, for water, the lower the temperature, larger is the density ratio between saturated liquid and vapor phases.

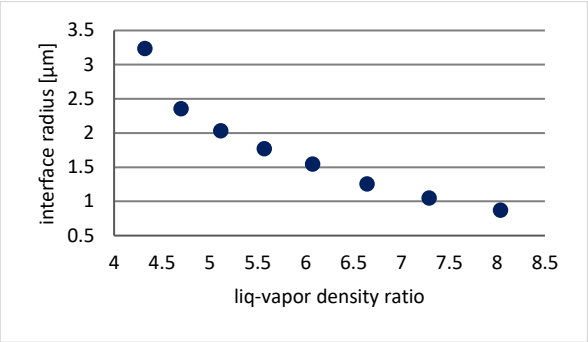


Figure 3. Saturated liquid-vapor interface radii for different density ratios

This verification of the model – however more conceptual than a strictly numerical one – makes possible further analyses of condensation in porous media filled with saturated fluid. In a domain similar to the previous one, but measuring 200x200 nm containing 50 nm diameter solids, the model was used with different distances between the solids, to check the relevance of this variable in the occurrence of capillary condensation. The results for three different channel sizes are showed in Fig. 4, considering T_r of 0.9.

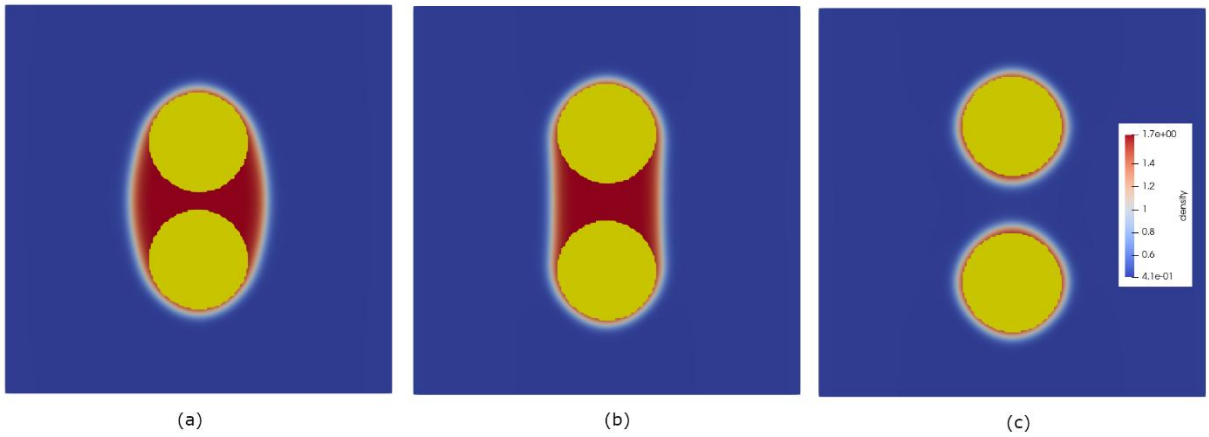


Figure 4. Condensation for Tr = 0.9 between solids for different distances: (a) 10 nm, (b) 20 nm, and (c) 30 nm.

As demonstrated, a certain minimal distance between the solid surfaces has to exist in order to the saturated liquid layers meet and coalesce. Otherwise, the saturated liquid layer adhered to the solid body will not be larger than the calculated interface thickness and capillary condensation in the porous medium does not take place.

5 Conclusions

It is possible to assert, based on the results, that for this particular LBM model the radius of the saturated liquid-vapor interface differs from one temperature to another, tending to agree with the Young-Laplace law. It is also possible to observe that the distance between solid bodies is a decisive factor on the presence of capillary condensation. Further analysis may uncover the characteristics of the interface and fluid flow when the borders are set with distinct density values.

Acknowledgements. The authors thank the CAPES – *Coordenação de Aperfeiçoamento de Pessoal de Nível Superior* – of the Ministry of Education of Brazil, Brazilian Council for Research (CNPq) and Pontifical Catholic University of Paraná (PUCPR) for the financial support.

Authorship statement. The authors hereby confirm that they are the sole liable persons responsible for the authorship of this work, and that all material that has been herein included as part of the present paper is either the property (and authorship) of the authors, or has the permission of the owners to be included here.

References

[1] P. C. Philippi, P. Rosendo Yunes, C. P. Fernandes and F. S. Magnani. "The microstructure of porous building materials: Study of a cement and lime mortar". *Transport in Porous Media*, vol. 14, pp. 219-245, 1994. https://doi.org/10.1007/BF00631003
[2] L. F. Dutra, N. Mendes and P. C. Philippi. "On the characterization of pore size distribution of building materials". *Journal of Building Physics,* vol. 41, n. 3, pp. 247-263, 2017. https://doi.org/10.1177/1744259117698515
[3] D. N. Siebert, P. C. Philippi and K. K. Mattila. "Consistent lattice Boltzmann equations for phase transitions". *Physical Review E,* vol. 90, n. 5, p. 053310, 2014. https://doi.org/10.1103/PhysRevE.90.053310
[4] H. Janssen. "Simulation efficiency and accuracy of different moisture transfer potentials". *Journal of Building Performance Simulation*, vol. 7, n.5, pp. 379-389, 2014. https://doi.org/10.1080/19401493.2013.852246
[5] R. Szijártó, A. Badillo, B. Ničeno and H.-M. Prasser. "Condensation models for the water–steam interface and the volume of fluid method". *International Journal of Multiphase Flow*, vol. 93, pp. 63-70, 2017. https://doi.org/10.1016/j.ijmultiphaseflow.2017.04.002
[6] S. M. Gatica, M. M. Calbi and M. W. Cole. "Simple model of capillary condensation in porous media". *Physical Review E*, vol. 65, n. 6, p. 061605, 2002. https://doi.org/10.1103/PhysRevE.65.061605
[7] A. G. Salinger and L. J. D. Frink. "Rapid analysis of phase behavior with density functional theory. I. Novel numerical methods". *Journal of Chemical Physics*, vol. 118, n. 16, pp. 7457-7465, 2003. https://doi.org/10.1063/1.1558313
[8] E. Shahraeeni and D. Or. "Pore-scale analysis of evaporation and condensation dynamics in porous media". *Langmuir*, vol. 26, n. 17, pp. 13924–13936, 2010. https://doi.org/10.1021/la101596y
[9] P. C. Philippi. *Thermodynamics: From Fundamentals to Multiphase and Multicomponent Systems*. Springer Cham, 2024.
[10] M. C. Sukop and D. Or. "Lattice Boltzmann method for modeling liquid-vapor interface configurations in porous media". *Water Resources Research*, vol. 40, p. W01509, 2004. https://doi.org/10.1029/2003WR002333
[11] S. Dou, L. Hao and H. Liu. "A mesoscopic model for simulating the physisorption process in nanopores". *Chemical Engineering Science*, vol. 262, p. 117988, 2022. https://doi.org/10.1016/j.ces.2022.117988
[12] J. Sodagar-Abardeh, A. Asadollahi and T. Loimer. "Mesoscale simulation of the equilibrium state of the confined nanoscale two-phase flow in the presence of corner interface and adsorbed liquid layer". *Chemical Engineering Science*, vol. 270, p. 118563, 2023. https://doi.org/10.1016/j.ces.2023.118563
[13] B. B. Kazemian, Q. Guo and P. Cheng. "Direct numerical simulations of moisture transport in porous media by a multi-component/phase-change lattice Boltzmann method". *International Journal of Heat and Mass Transfer*, vol. 176, p. 121264, 2021. https://doi.org/10.1016/j.ijheatmasstransfer.2021.121264
[14] J. Li, W. Zheng and F. Hong. "Three-dimensional lattice Boltzmann investigation on pore scale liquid–vapor distribution patterns and heat transfer performance of a loop heat pipe heterogeneous porous wick evaporator". *International Communications in Heat and Mass Transfer*, vol. 128, p. 105639, 2021. https://doi.org/10.1016/j.icheatmasstransfer.2021.105639
[15] X. Shan and H. Chen. "Lattice Boltzmann model for simulating flows with multiple phases and components". *Physical Review E,* vol. 47, n. 3, pp. 1815-1820, 1993. https://doi.org/10.1103/PhysRevE.47.1815
[16] L. Chen, Q. Kang, Y. Mu, Y.-L. He and W.-Q. Tao. "A critical review of the pseudopotential multiphase lattice Boltzmann model: Methods and applications". *International Journal of Heat and Mass Transfer* vol. 76, pp. 210-236, 2014. https://doi.org/10.1016/j.ijheatmasstransfer.2014.04.032.
[17] X. He and L.-S. Luo. "Theory of the lattice Boltzmann method: From the Boltzmann equation to the lattice Boltzmann equation". *Physical Review E,* vol. 56, n. 6, pp. 6811-6817, 1997. https://doi.org/10.1103/PhysRevE.56.6811
[18] P. C. Philippi, L. A. Hegele Jr., L. O. E. dos Santos and R. Surmas. "From the continuous to the lattice Boltzmann equation: The discretization problem and thermal models". *Physical Review E*, vol. 73, n. 5, p. 056702, 2006. https://doi.org/10.1103/PhysRevE.73.056702
[19] X. Shan, X.-F. Yuan and H. Chen. "Kinetic theory representation of hydrodynamics: a way beyond the Navier–Stokes equation". *Journal of Fluid Mechanics*, vol. 550, pp. 413-441, 2006. https://doi.org/10.1017/S0022112005008153
[20] P. L. Bhatnagar, E. P. Gross and M. Krook. "A model for collision processes in gases. I. Small amplitude processes in charged and neutral one-component systems". *Physical Review*, vol. 94, n. 3, pp. 511-525, 1954. https://doi.org/10.1103/PhysRev.94.511
[21] D. N. Siebert, L. A. Hegele Jr. and P. C. Philippi. "Lattice Boltzmann equation linear stability analysis: Thermal and athermal models". *Physical Review E*, vol. 77, n. 2, p. 026707, 2008. https://doi.org/10.1103/PhysRevE.77.026707
[22] Q. Zou and X. He. "On pressure and velocity boundary conditions for the lattice Boltzmann BGK model". *Physics of Fluids*, vol. 9, n. 6, pp. 1591-1598, 1997. https://doi.org/10.1063/1.869307